Developing Etching Process for Nanostructures on InGaP and AlInP Using OX-35 Etcher

Jieyang Jia, Li Zhao

Mentors: Mary Tang, James McVittie

I. INTRODUCTION

Nanostructures have been widely applied to solar cells for antireflection coating, light trapping enhancement, and so forth [1]. In 2013, D. Liang et al. at Stanford University has demonstrated the use of nanostructured AlGaAs window layer to increase the performance of GaAs solar cells. Although it has been demonstrated that the nanostructure AlGaAs window layer can enhance the photocurrent, open-circuit voltage (Voc) and fill factor (FF), it was also noted that the major loss mechanism in the cell is surface recombination on the nanostructure surface. Since the nanostructure is usually formed by dry etching, surface damage is inevitable, which results in the increase of surface recombination. To cope with this challenge, InGaP materials are considered as potential substitutes since they usually have much lower surface recombination($\sim 4 \times 10^4 cm\ s^{-1}$) than AlGaAs materials($\sim 9 \times 10^5 cm\ s^{-1}$) [2]. On the other hand, the high refractive index of III-V semiconductor materials such as InGaP and AlGaAs results in optical reflection loss up to 36% for the incident light [3], thus generates the need to form nanostructures to reduce the optical loss. Therefore, it is of great research interests to investigate the dry etch process nanostructures on III-V materials such as InGaP.

Beside InGaP, AlInP nanostructures are also of great research interests due to their applications as the window layer of multi-junction solar cells. In addition, due to the larger direct band gap (2.3eV), AlInP is extensively adopted in the mass production of the high-brightness light-emitting diodes[4]. The wave-guiding effect caused by AlInP nanostructures leads to better light extraction from bulk material, thus increases the overall LED efficiency.

In SNF, we have demonstrated InGaP nanostructure etching using PQuest. However, the etching process had showed limited etching rate and unsatisfactory process variation. With Ox-

35 etcher we hope to get faster and more controllable etching rate, larger selectivity and smaller process variation. In addition, the etching temperature of Ox-35 will be much lower than that of PQuest, which allows us to use photoresist as the mask for calibration, and thereby simplifies the calibration process.

In this project, we calibrated etching processes for 4 different materials: InP, SiO2 nanospheres, InGaP, and AlInP. This is the first time in SNF that the InGaP and AlInP etching process was systematically studied on Ox-35 etcher, therefore the information from this project will potentially be very helpful for SNF and future Ox-35 users. In addition, this project not only helps us make better InGaP and AlInP nanostructures, but also enhances our understanding of III-V drying etching process and enable us to better utilize the SNF resources for III-V nanostructure research.

II. METHODOLOGY

This project was divided into two phases. First, we investigated the etching rate, conformity and other process parameters of InP, AlInP, InGaP, and SiO2 nano-spheres. With the results from such calibration, we then proceeded to nanostructures etching on different materials.

1. Etching rate and conformity calibration

In the first phase, we designed a process flow to calibrate the etching rate and conformity, as shown in Fig.1.

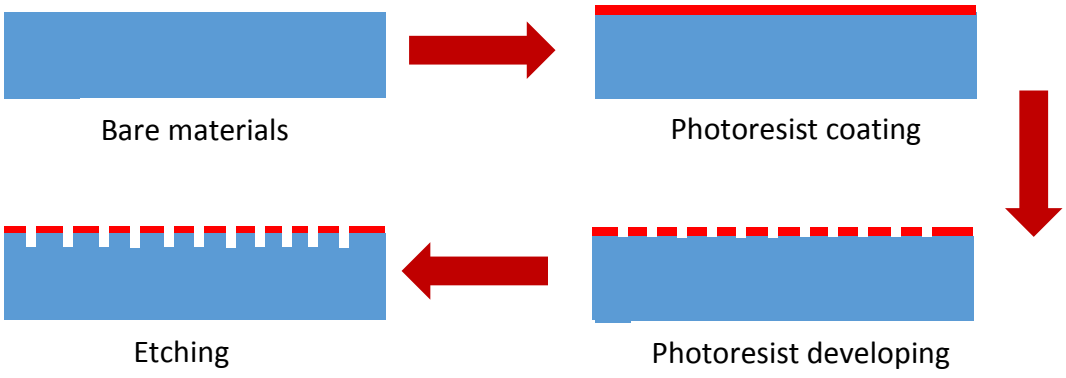

Figure. 1: Process flow for the etching rate and conformity calibration.

Since all the materials are in pieces, we used Headway to coat the 3612 photoresist, then Karlsuss Aligner to do the expose, and Headway again to do the developing.

2. Nanostructures etching process calibration

In the second phase, we designed a process flow to calibrate the nanostructure etching, as shown in Fig.2:

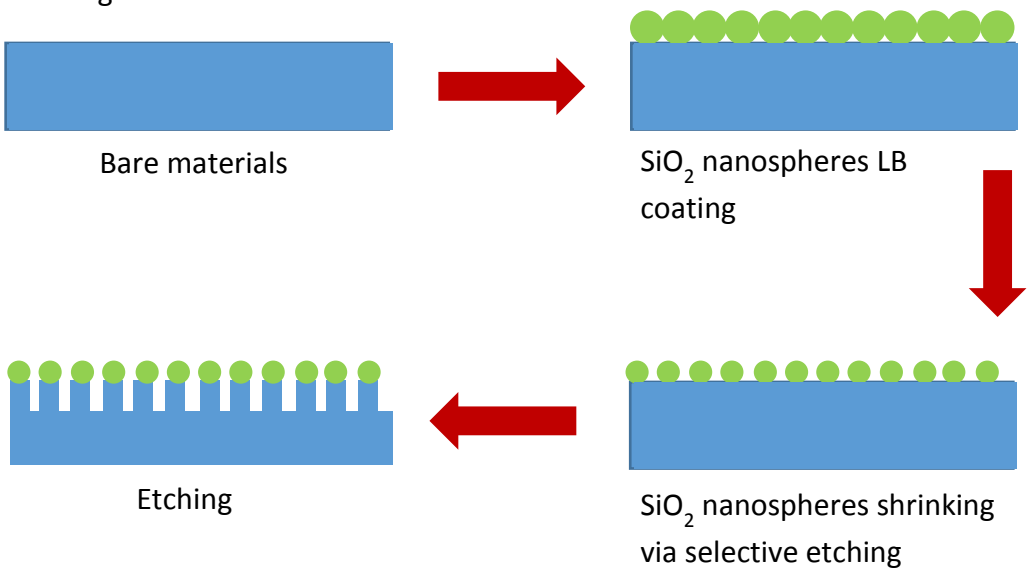

Figure. 2: Process flow for the nanostructure etching calibration.

In both phases, the starting recipe is the InP low etching rate recipe (referred as Low ER) in OX-35. The CH4/H2 gas mixture was used to etch InP, InGaP, and AlInP, since CH4 will balance the removal of In and P.[5] However, due to the problem of polymer byproducts in this low etching rate recipe, another recipe with Cl2/CH4/H2 gas mixture (referred as High ER) has also been investigated. [7] The addition of Cl2 also facilitated the etching of Ga and Al base material.[6] For the Cl2/CH4/H2 based recipe, we also decreased the DC power to increase the undercut below the nano-spheres. Then we tried increasing the pressure to increase the undercut, and tuned the Cl2 flow a bit to investigate the tuning of physicality.

For the SiO_2 nano-sphere etching, we tried the chamber clean recipe based on O2/SF6. Etching of SiO2 using recipes mentioned above for III-V etching was also performed, in order to investigate the selectivity between the SiO2 mask and the bulk material. Please refer to Appendix. I for the key parameters of all the recipes mentioned above.

We used pieces of an InP wafer for the InP process. For InGaP and AlInP process, we used pieces of 500nm epitaxial $In_{0.5}Ga_{0.5}P$ and $Al_{0.5}In_{0.5}P$ on GaAs substrates. The size of a typical starting sample is shown in Fig. 3. The actual etched samples were cut into smaller pieces.

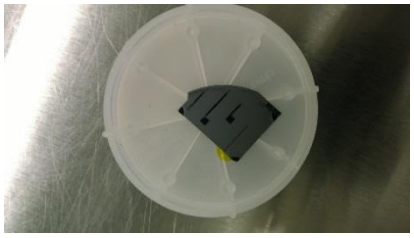

Figure. 3: InP starting sample. Similar size for AlInP and InGaP.

III. RESULTS

The etching and conformity of InP, InGaP, AlInP, and SiO_2 nanospheres with CH4/H2 and Cl2/CH4/H2 processes have been investigated. In this section, the most important results of each materials are discussed. The detailed and comprehensive etching results are listed in Appendix II.

1. InP

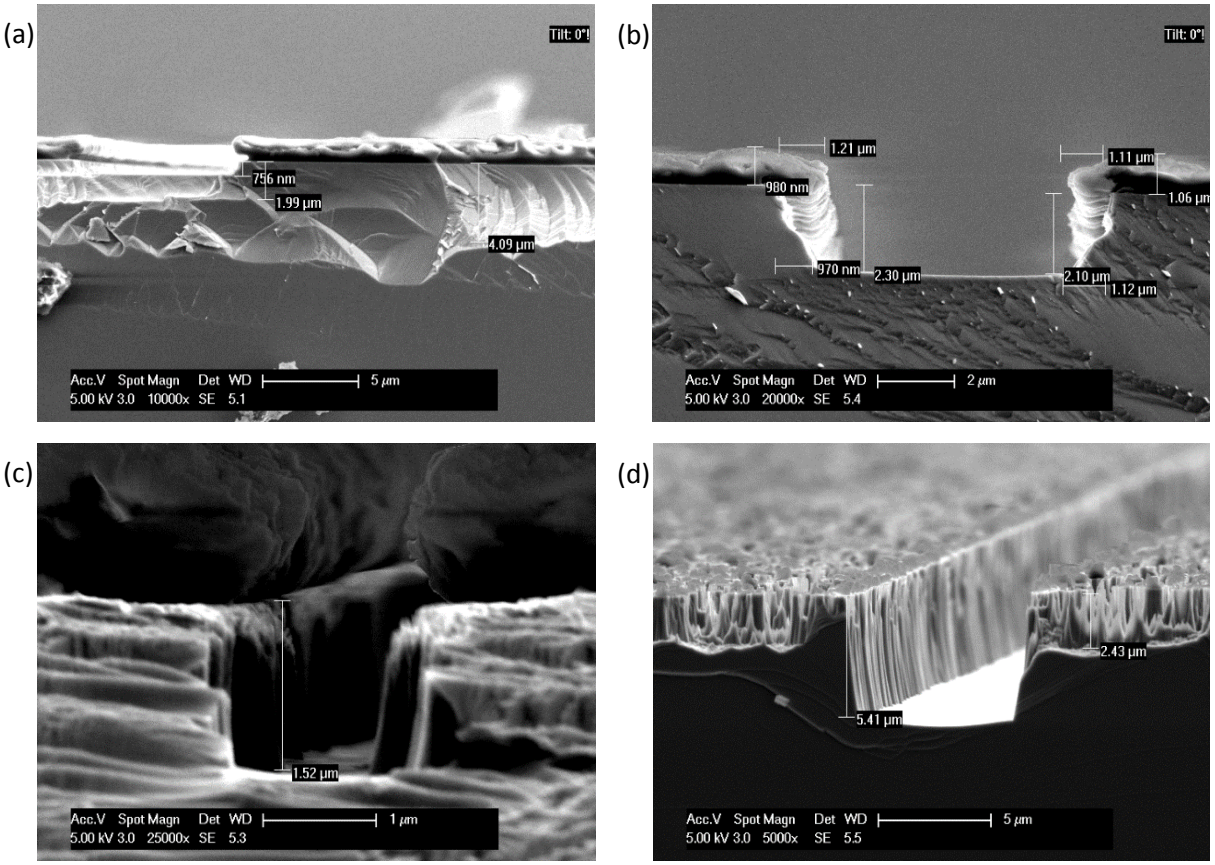

Figure. 4: SEM images of InP etching with photoresist mask. (a) Low ER, 5 min; (b) Low ER, 15 min; (c) High ER, 2 min; (d) High ER, 5min.

Etching rate of Low ER recipe on InP is 154.4nm/min, the sidewall angle is 67.3˚, the bottom is very smooth. Significant polymer formation has been observed.

Etching rate of High ER recipe is around 750nm/min, photoresist has been etched away with 5mins etching. The etching is almost vertical, the bottom is smooth, but the sidewall is not perfectly smooth which may be due to the photoresist on top.

2. InGaP

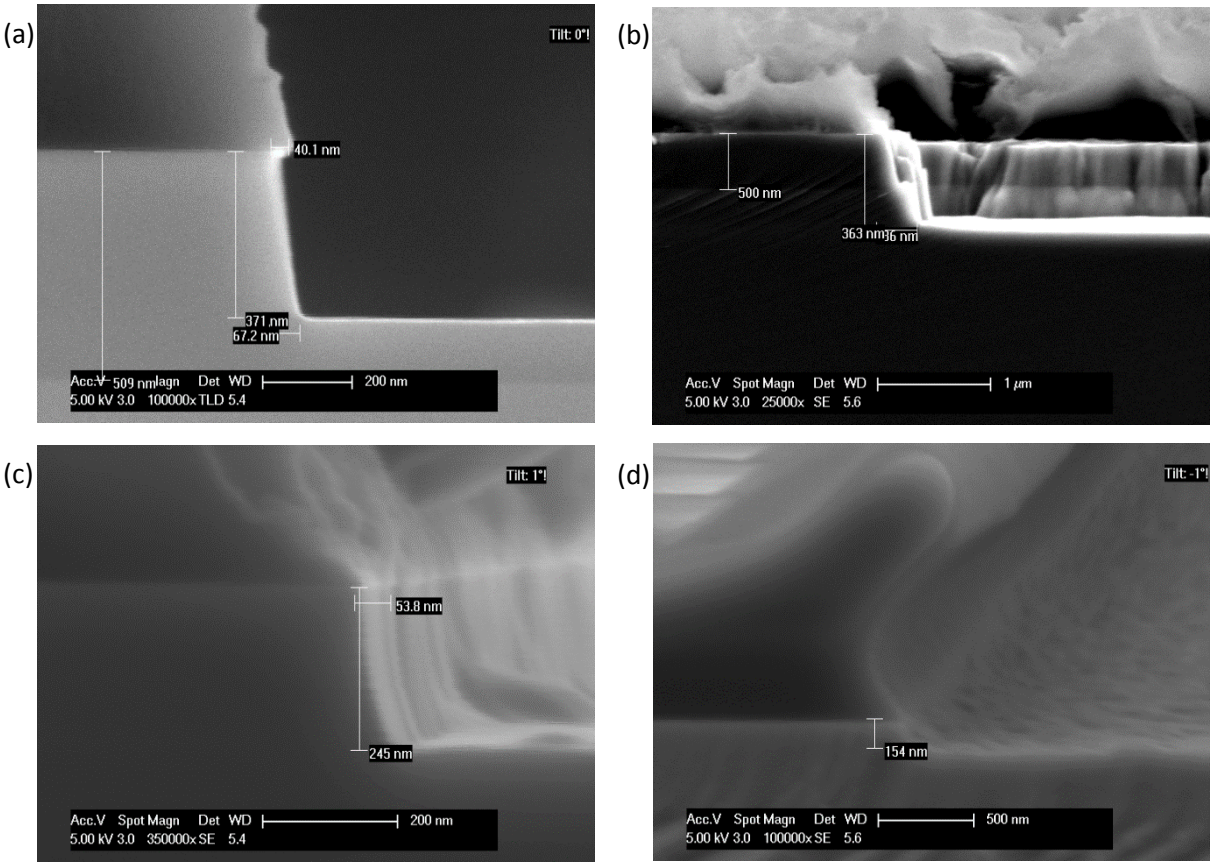

Figure. 5: SEM images of InGaP etching with photoresist mask. (a) Low ER, 5 min; (b) High ER,75W 4mT, 2min; (c) High ER, 25W 4mT, 60s; (d) High ER, 25W 8mT, 60s.

We tried the Low ER recipe for InGaP etching, as shown in Fig.5 (a), the etching rate was around 70nm/min. The sidewall and bottom were both smooth. Undercut was negligible.

When using the High ER 75W 4mT recipe, the etching rate was too fast that the top 500nm InGaP layer was etched through in less than 2 minutes. Then we reduced the DC power to 25W, which lowered the etching rate to around 240nm/s. With this recipe the undercut was negligible, but the sidewall and bottom were not very smooth. To increase the undercut, we increased the pressure to 8mT, as shown in Fig.5 (d), the undercut increased a significantly, with etching rate decreased to 178nm/min.

3. AlInP

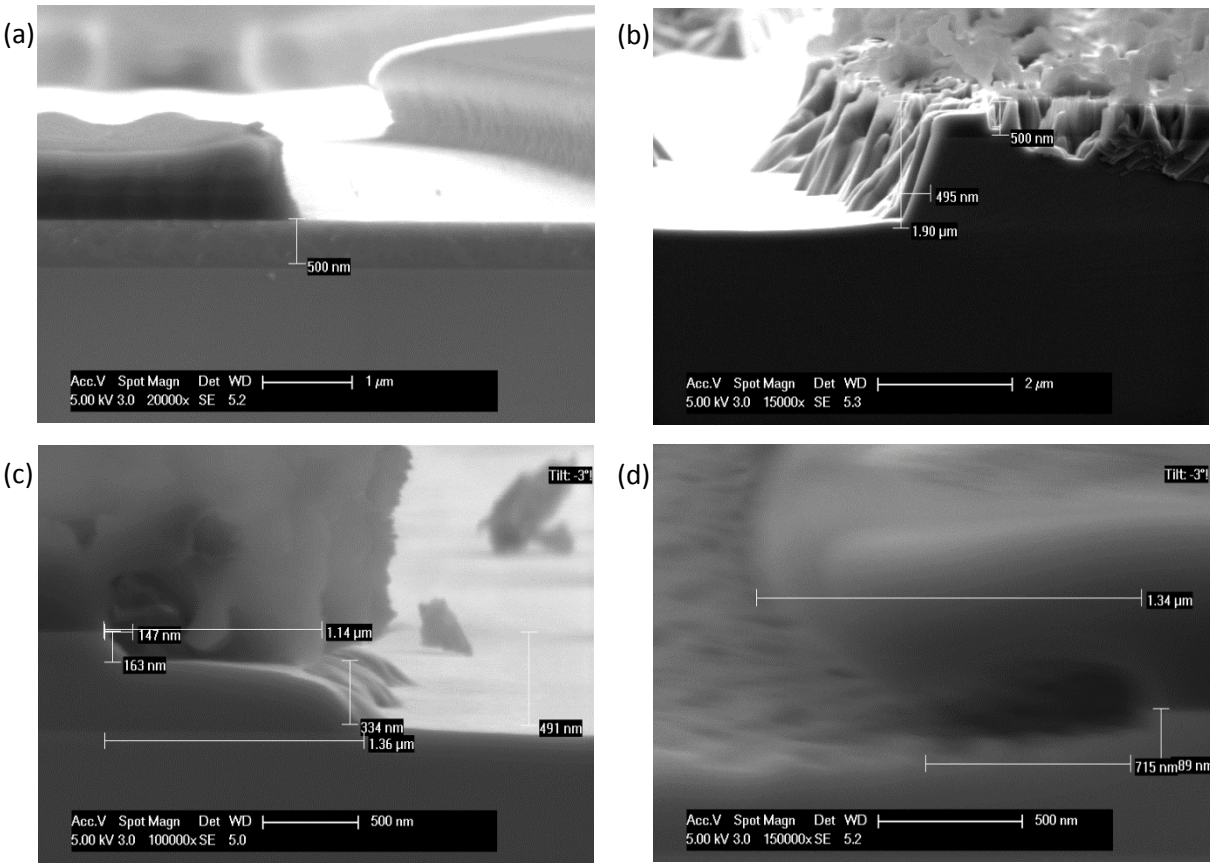

Figure. 6: SEM images of AlInP etching with photoresist mask. (a) Low ER, 3 min; (b) High ER,75W 4mT, 5min; (c) High ER, 25W 4mT, 60s; (d) High ER, 25W 8mT, 60s.

As shown in Fig.6 (a), AlInP was not etched at all in at least 3 min when we used Low ER, which might be due to the aluminum oxide on the surface.

For the High ER 75W 4mT recipe, the etching rate is too fast, so we turned the DC power down to 25W, which decreased the etching rate to around 428nm/min. With 25W DC power, the plasmas was less directional, resulting in larger undercut. The etched surface was not very smooth. To further increase the undercut, we changed the pressure to 8mT, as shown in Fig.6 (d), the etching rate decreased to 90 nm/min, and the undercut increased to 1340nm. The surface was still very rough.

4. SiO_2

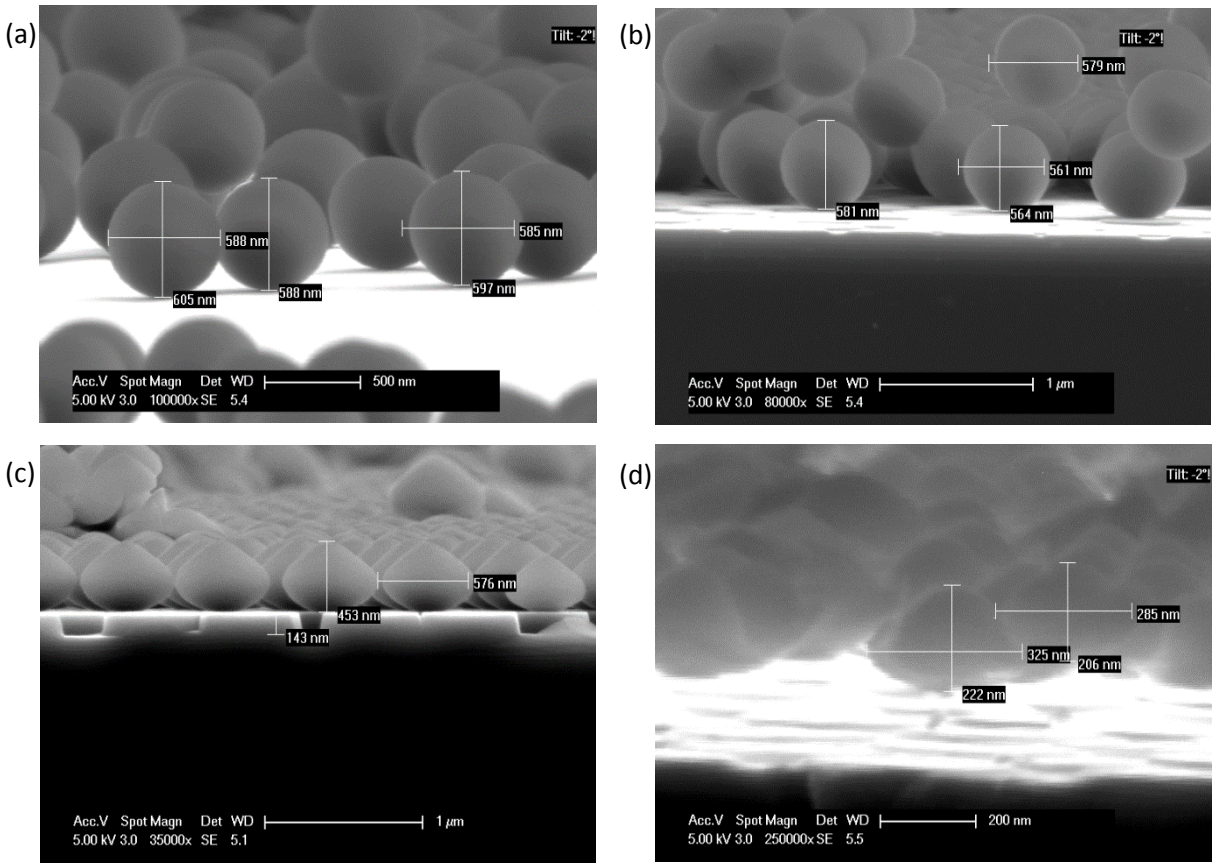

Figure. 7: SEM images of SiO2 sphere etching. (a) before etching; (b) High ER, 25W 4mT, 30s (c) High ER, 75W 4mT, 2 mins; (d) High ER, 25W 8mT, 60s.

To etch the nanostructures, the ball shrinking process is critical. We first investigated the SiO_2 nanosphere etching process by using High ER not Low ER. As it is shown in Fig.7 (a), with High ER 25W 4mT and 8mT recipes, the nanospheres were not etched noticeably. However when we increased the power to 75W, the nanospheres started to be etched due to higher physicality. The etching rate in lateral direction is ~2 nm/min, and the etching rate in vertical direction is around 70nm/min.

To further shrink the SiO_2 nanospheres, the Chamber Clean Recipe(SF6/O2) was attempted. SF6 was shown to be a good oxide etching gas. The etching rate increased to 300nm/min in lateral direction, 400nm/min in vertical direction.

5. InGaP Nanostructures

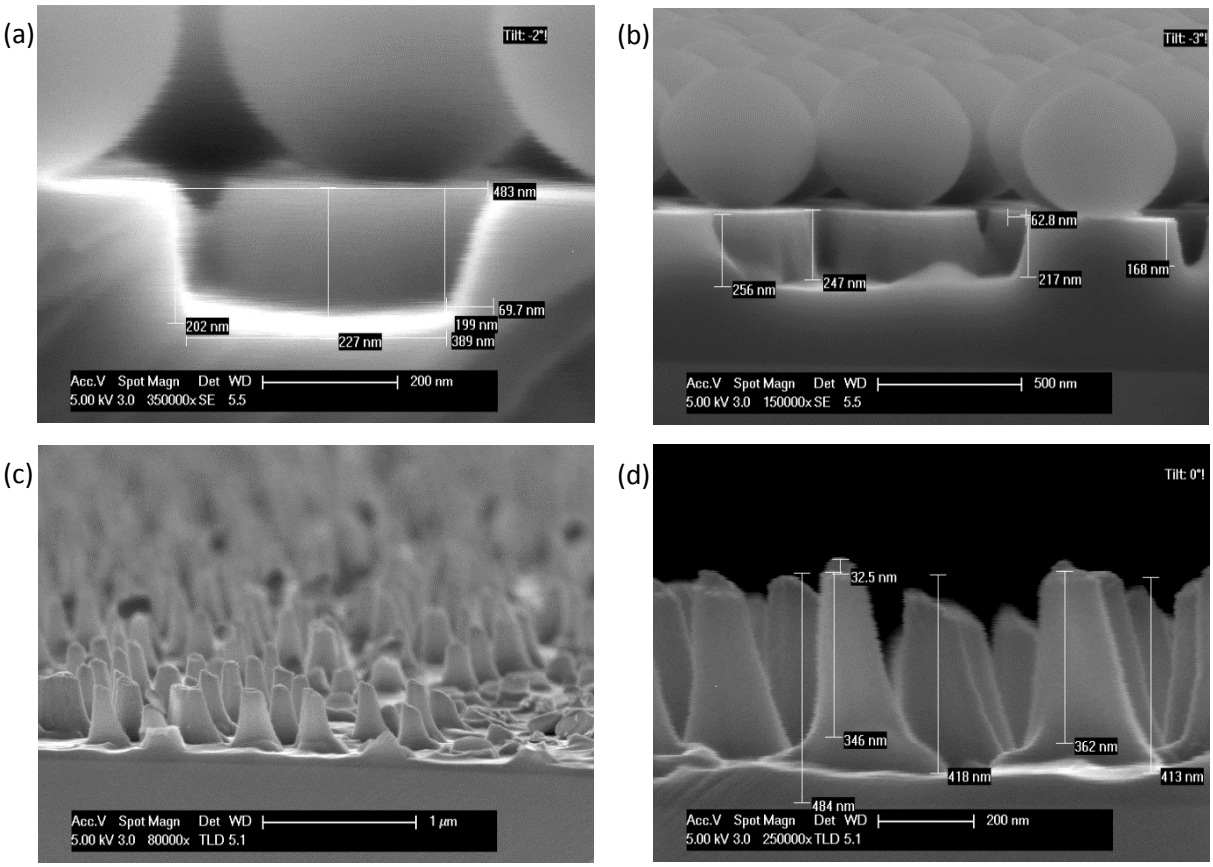

Figure. 8: SEM images of InGaP nanostructures etched with High ER. (a) 25W 2mT, 2 min; (b) 25W 4mT, 1 min; (c)(d) 25W 8mT, 2 min. (a) (b) were etched without 1 min SiO2 ball shrinking, (c)(d) were etched with 1 min ball shrinking.

Finally we explored the nanostructure etching process. As the High ER recipes generated more controllable results, we tuned the High ER recipe only. The results of High ER 25W 2mT without ball shrinking is shown in Fig.8 (a), the etching rate was around 100nm/min, and slope of the side wall was very large. To have a smaller slope, we increased the pressure to 4mT, then the slope decreased, making the structure more like a cone. The etching rate also increased to 250nm/min, whichwa consistent with the etching rate we calibrated previously with photoresist mask. To increase the undercut further, we changed pressure to 8mT.

By shrinking the nanospheres for 1 min before High ER etching, we were able to generate very promising nanostructures. After 2mins High ER etching, we generated nanocone structures with 415nm in height, and with a sharp top, as shown in Fig.8 (c) and (d).

6. AlInP nanostructures

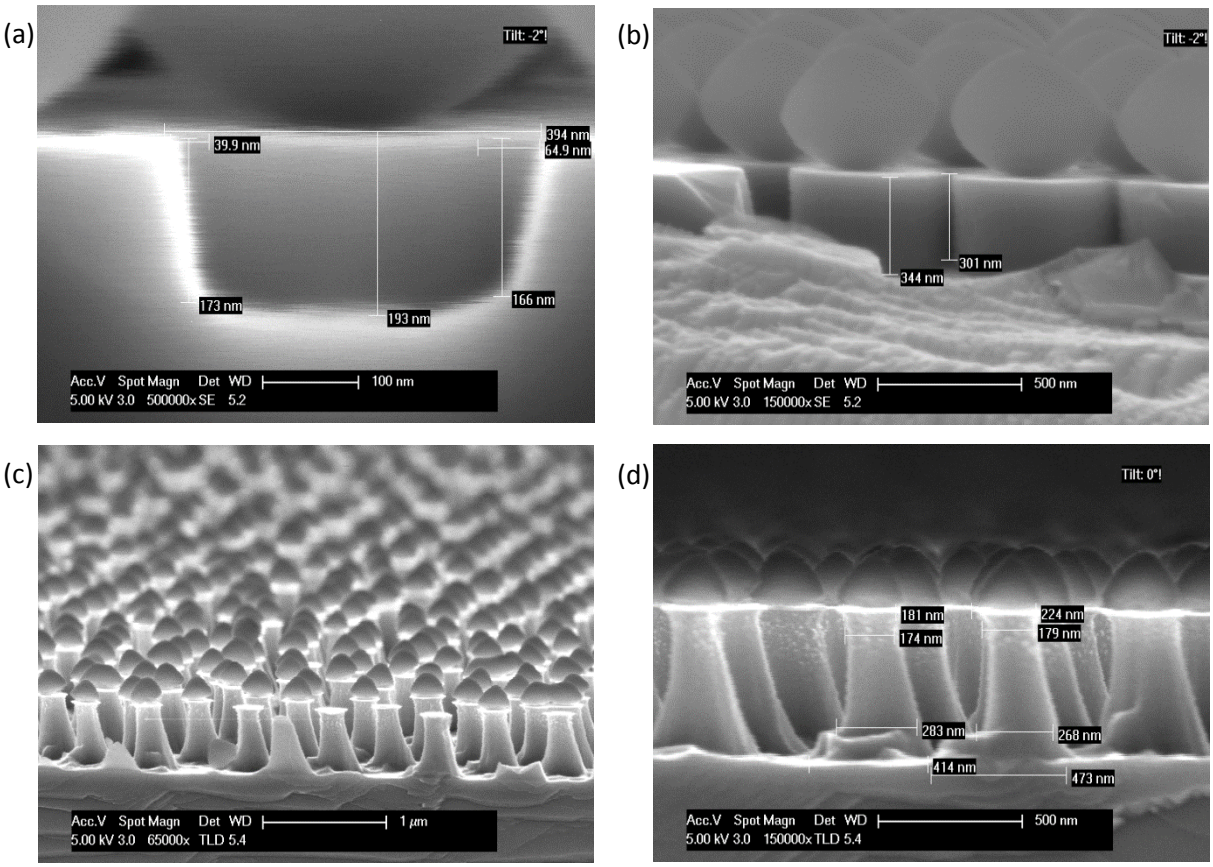

Figure. 9: SEM images of AlInP nanostructures etched with High ER. (a) 25W 2mT, 2 min; (b) 25W 4mT, 1 min; (c)(d) 25W 8mT, 2 min. (a) (b) were etched without 1 min SiO2 ball shrinking, (c)(d) were etched with 1 min ball shrinking.

The similar trend to InGaP was observed on AlInP nanostructure etching. Using High ER 25W, 4mT was not good enough as the structure wall was very vertical, as shown in Fig.9 (b). Again 8mT generated the best results.

With 1min of nanosphere shrinking, the etching rate with High ER, 25W 8mT was around 250nm/min. The top width of the structure was around 175nm, and the bottom width was around 400nm. The nanospheres were shrunk to around 200nm in width. Due to the high selectivity between SiO_2 and AlInP, nanocone structures were achieved.

IV. DISCUSSION AND CONCLUSION

We investigated the AlInP and InGaP nanosture etching process using OX-35 etcher. Two different series of etching recipes have been investigated. The key parameters of all the recipes are listed in Appendix I.

For the Low ER recipe, the CH4/H2 gas etched InP very well, the sidewall and bottom are very smooth and conformity are very good. This recipe also etched InGaP well, generating very smooth sidewall. However, AlInP was not etched by Low ER recipe at all. We hypothesize that the reason might be due to the top oxide layer which does not react with CH4/H2. This recipe did not etching SiO_2 nanospheres as well.

The focus of our calibration effort was on the High ER recipes. The results were consistent with what we expected. The etching rates of InP and InGaP were increased to around significantly, and AlInP was also etched successfully.

After tuning the RF power and pressure to control the etching rate and conformity, we concluded that High ER, 25W 8mT recipe was the best for nanostructure etching. We were able to generate short nano-pillars using this recipe with SiO2 nanosphere as the mask. With the addition of a SiO2 nanosphere shrinking process prior to the material etching, we were able to generate very promising nanostructures. We also attempted tuning the chemical composition of the etchant gas, however due to limited time and resource we were not able to complete this part of the project, and the preliminary results were not verified. Therefore we decided to omit this part from this report to avoid confusion for future users.

In conclusion, in this work we have systematically studied the etching process of 4 different materials with 2 series of recipes. We also successfully demonstrate nanostructrues on InGaP and AlInP surfaces. This project not only enables us to fabricate better nanostructures, but also deepened our understanding on plasma etching of III-V materials. We hope that the results and insights from this project can be helpful to SNF staff and future users of Ox-35.

Acknowledgements

We thank Mary Tang and James Mvittie for helping us develop the recipes on OX-35 etcher. We thank to Yusi Chen to do the LB SiO_2 nanosphere coating. We also thank OEpic for providing us with the precious InP, InGaP, and AlInP materials.

References

1. Dong Liang, Yangsen Kang, Yijie Huo, Yusi Chen, Yi Cui, and James S. Harris. *Nano Letters* **2013**, *13* (10), 4850-4856

2. S. J. Pearton, F. Ren, W. S. Hobson, C. R. Abernathy, R. L. Masaitis, U. K. Chakrabarti. *Applied Physics Letters*, **1993,** vol. 63, issue. 26, 3610-3612.

3. Nguyen Dinh Lam, Youngjo Kim, Kangho Kim, and Jaejin Lee. *Journal of Nanomaterials*, **2013**, 13(785359), 6 pages

4. H. C. Wang, Y. K. Su, C. L. Lin, W. B. Chen, and S. M. Chen. *IEEE Photonics Technology Letters, Vol.14, No.11, 2002*

5. S. Guilet and S. Bouchoule, C Jany, C. S. Corr, and P. Chabert. *American Vacuum Society, DOI:10.1116/1.2348728*

6. J. Hong, E. S. Lambers, C. R. Abernathy, S. J. Pearton, R. J. Shul, and W. S. Hobson, *Journal of Electronics materials, Vol. 27, No.3, 1998*

7. Lee Chee-Wei and Chin Mee-Koy, *CHIN.PHYS.LETT, Vol.23, No.4, 903, 2006*

Appendix I. Key Parameters of Recipes

	Low ER	High ER, 75W 4mT	High ER, 25W 4mT	High ER, 25W 2mT	High ER, 25W 8mT	Chamber Clean
Chamber pressure(mT)	10	4	4	2	8	20
DC power(W)	120	75	25	25	25	70
ICP power(W)	350	2000	2000	2000	2000	2000
Cl2 flow(sccm)	0	7	7	7	7	0
CH4 flow(sccm)	50	8	8	8	8	0
H2 flow(sccm)	10	5.5	5.5	5.5	5.5	0
SF6 flow(sccm)	0	0	0	0	0	20
O2 flow(sccm)	0	0	0	0	0	100

Appendix II. Detailed Etching Results

Material	Recipe	Etch Rate (vertical/lateral) (nm/min)	Undercut (nm/min)	Sidewall Angle (dec)	Smoothness (bottom/sidewall)	Photoresist Condition	Comments
InP	Low ER	154	81	67.3	Smooth/rough	Polymer observed	Significant polymer formation
	High ER, 75W 4mT	750	NA	>86	Smooth/zigzag	Degraded, porous	
	High ER, 25W 4mT	404	1500	51	Rough/rough	Degraded	
	High ER, 25W 2mT	NA	NA	NA	NA	NA	Etching failed
	High ER, 25W 8mT	269	<0	13.3	Rough/rough	Wavy, locally peeled	
InGaP	Low ER	70	8	84	Smooth/smooth	Polymer observed	Significant polymer formation
	High ER, 75W 4mT	>300	<0	>80	Smooth/zigzag	Degraded	Epi etched through
	High ER, 25W 4mT	240	<0	78	Rough/mild zigzag	Degraded	
	High ER, 25W 2mT	192	NA	75.3	Smooth/smooth	NA	SiO2 mask
	High ER, 25W 8mT	178	300	39	Very rough/very rough	Wavy	
AlInP	Low ER	<5	NA	NA	NA	NA	No etching observed
	High ER, 75W 4mT	>300	NA	NA	Smooth/zigzag	Porous	Epi etched through
	High ER, 25W 4mT	428	1140	varying	Smooth/rough	Porous	
	High ER, 25W 2mT	365	NA	82	Smooth/smooth	NA	SiO2 mask
	High ER, 25W 8mT	90	1340	7.1	Very rough/very rough	Wavy	
SiO2	Low ER	<5	NA	NA	NA	NA	No etching observed
	High ER, 75W 4mT	70/2	NA	NA	NA	NA	
	High ER, 25W 4mT	<50/<50	NA	NA	NA	NA	
	High ER, 25W 2mT	<50/<50	NA	NA	NA	NA	
	High ER, 25W 8mT	<50/<50	NA	NA	NA	NA	
	Chamber Clean	400/300	NA	NA	NA	NA	

NA = data not available